Materials Letters 165 (2016) 95–98

Contents lists available at ScienceDirect

Materials Letters

journal homepage: www.elsevier.com/locate/matlet

Relationship between the Ca/P ratio of hydroxyapatite thin films and the spatial energy distribution of the ablation laser in pulsed laser deposition

Hiroaki Nishikawa [a,*], Tsukasa Hasegawa [b], Akiko Miyake [c], Yuichiro Tashiro [c], Yoshiya Hashimoto [d], Dave H.A. Blank [e], Guus Rijnders [e]

[a] Faculty of Biology-Oriented Science and Technology, Kinki University, 930 Nishi-Mitani, Kinokawa, Wakayama 649-6493, Japan
[b] Graduate School of Biology-Oriented Science and Technology, Kinki University, 930 Nishi-Mitani, Kinokawa, Wakayama 649-6493, Japan
[c] Department of Removable Prosthodontics and Occlusion, Osaka Dental University, 8-1 Kuzuha-Hanazano, Hirakata, Osaka 573-1121, Japan
[d] Department of Biomaterials, Osaka Dental University, 8-1 Kuzuha-Hanazono, Hirakata, Osaka 573-1121, Japan
[e] MESA+ Institute for Nanotechnology, University of Twente, 7500 AE Enschede, The Netherlands

ARTICLE INFO

Article history:
Received 6 October 2015
Received in revised form
19 November 2015
Accepted 25 November 2015
Available online 27 November 2015

Keywords:
Pulsed laser deposition
Hydroxyapatite
Laser spot size
Ca/P ratio
Biomaterial

ABSTRACT

Variation of the Ca/P ratio in hydroxyapatite ($Ca_{10}(PO_4)_6(OH)_2$) thin films was studied in relation to the spot size of the ablation laser for two different spatial energy distributions in pulsed laser deposition. One energy distribution is the defocus method with a raw distribution and the other is the projection method without the weak portion at the edges of the ablation laser spot. A Ca/P ratio closer to that of stoichiometry was obtained with the larger spot sizes for both methods, and with the projection method compared to the defocus method. It is considered that a more uniform spatial energy distribution of the ablation laser improves the Ca/P ratio.

1. Introduction

Hydroxyapatite (HA), $Ca_{10}(PO_4)_6(OH)_2$, is widely applied in medical and dental devices [1–5] because of its excellent bone conduction property. To prepare high quality HA thin films, we have chosen pulsed laser deposition [6–8] (PLD) due to the similarity between the chemical compositions of the target and the thin film in general from among various coating techniques [2,3,9–14]. It has been found, however, that the Ca/P ratio deviates drastically from the stoichiometric value on HA thin films prepared via PLD [8]. Because the Ca/P ratio is critical to govern the solubility of HA in a living body [15], the stoichiometric Ca/P ratio of the HA thin film is quite important. To improve the Ca/P ratio of HA thin films, we noted "spot size" which is an area of the ablation laser on the target surface, because some studies reported an effect of the spot size [16–18]. However, a systematic dependence of the chemical composition upon the spot size has not been reported. Recently, we found that a larger spot size clearly improved the Ca/P ratio [19]. To find the factor with respect to the relationship between the spot size and the Ca/P ratio, in this work, we noted the spatial energy distribution of the ablation laser because the spatial energy distribution of the ablation laser causes the fluence (area density of the laser energy) on the target surface to be distributed spatially [20]. If the Ca/P ratio depends upon the fluence of each spatial position [19], different spot sizes will result in a variation of the Ca/P ratio via the different spatial energy of the ablation laser at each position in the distribution. In this study, we report the dependence of the Ca/P ratio upon the spot size and the spatial energy distribution of an ablation laser with a constant fluence.

2. Experimental details

HA thin films were deposited on Al_2O_3 (0001) single-crystal substrates (K&R Creation; $10 \times 10 \times 0.5$ mm^3, front-side polished) via PLD. A KrF excimer laser (Lambda Physik; COMPex 102, FWHM of typical pulse duration = 20 ns) was used and the pulse repetition rate was 10 Hz. The ablation laser was focused onto the target surface by a biconvex lens consisting of synthesized silica (Sigmakoki; SLSQ-50B-150P, focal length = 137.10 mm and measured transmittance = ~0.95) with an incident angle of 45°, where the

* Corresponding author.
E-mail address: nishik32@waka.kindai.ac.jp (H. Nishikawa).

http://dx.doi.org/10.1016/j.matlet.2015.11.115
0167-577X/

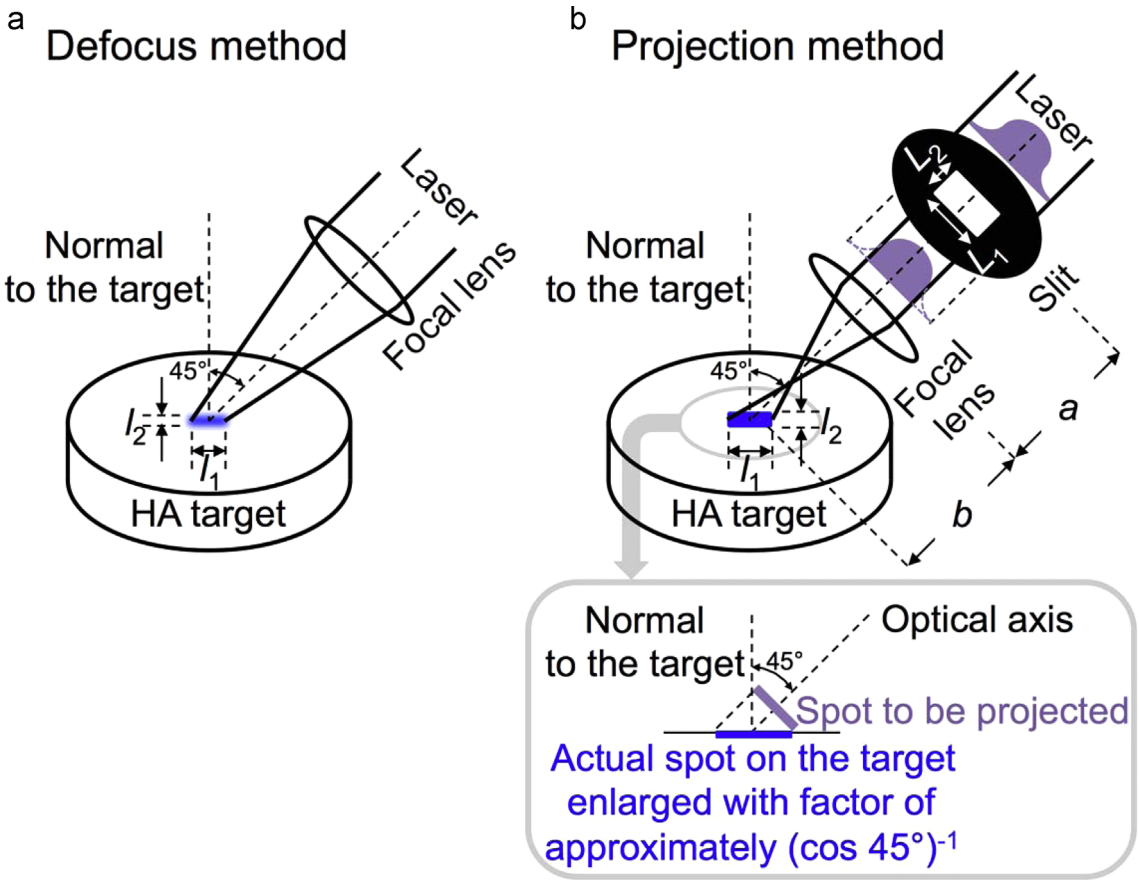

Fig. 1. Schematics of the methods used to control the spot size and the spatial energy distribution of an ablation laser with a constant fluence. (a) The defocus method, wherein the spot size (*ss*) is calculated with the equation $ss = l_1 l_2$, and l_1 and l_2 are measured with a vernier caliper. (b) The projection method, wherein the spot on the target surface is sharply projected and *ss* is calculated with the thin lens equation given in (Eqs. (1) and 2). See text for a detailed discussion.

ablation laser passed through a synthesized silica window (measured transmittance = ~0.95). The target was a commercially available HA pellet (HOYA Technosurgical; Pentax CELLYARD™, purity ≥ 99%), where the distance between the target and the substrate was 38 mm and the substrate was kept at 400 °C during the growth of the HA thin films, monitored by an optical pyrometer (Chino; IR-CI2SCF). An $O_2 + H_2O$ gas mixture was generated by bubbling pure O_2 gas though a distilled water bath and the gas mixture was introduced into the growth chamber at a pressure of 50 Pa.

In this study, we examined two methods, named the "defocus method" and the "projection method", to control the spot size and the spatial energy distribution of the ablation laser. The defocus method was the same as that used in our previous study, which consists simply of changing the distance between the target and the focal lens [19]. After the lens position was fixed, the target was pre-ablated and the two sides of the dent area, i.e., the spot size (*ss*), were measured using a vernier caliper for each lens position, which is schematically shown in Fig. 1(a) wherein $ss = l_1 l_2$. The projection method is schematically illustrated in Fig. 1(b), where *f* is the focal length of the lens, *a* is the distance between the rectangular slit and the focal lens, and *b* is the distance between the focal lens and the target surface. The ablation laser was passed through a slit to remove the weak portion of the ablation laser, as shown in Fig. 1(b). The slit shape was projected onto the target surface with clear edges in such a way that the thin lens equation was satisfied, which is given as

$$\frac{1}{f} = \frac{1}{a} + \frac{1}{b}. \tag{1}$$

The *ss* was controlled with the equation of magnification (*m*) given as

$$m = \frac{l_1}{L_1} = \frac{l_2}{L_2} = \frac{b}{a}, \quad ss = l_1 l_2 = \frac{m^2 L_1 L_2}{\cos 45^\circ} \tag{2}$$

where L_1 and L_2 are the two sides of the rectangular slit ($L_1 = 2$ cm and $L_2 = 1$ cm in this study) and l_1 and l_2 are the two sides of the projected ablation laser on the target. The positions of the slit and the focal lens were chosen to obtain the spot size calculated using the value of *m* on the basis of (Eqs. (1) and 2). The factor $(\cos 45^\circ)^{-1}$ comes from the angle of 45° between the optical axis of the ablation laser and the target surface, as illustrated in the bottom of Fig. 1(b). For both methods, the total laser energy (*E*) was measured using an energy meter (Coherent; J-50MUV-248, 7.365V/J) placed just in front of the focal lens. The *E* was adjusted to ensure constant values of the fluence (*F*), calculated using

$$F = \frac{E \times 0.95 \times 0.95}{ss}, \tag{3}$$

where the two factors of 0.95 are the transmittances of the focal lens and the window, and used to calculate a net energy on the target. Before the thin film deposition, the target surface was pre-ablated for 1500 shots.

The thickness of the prepared HA thin film was measured using a stylus surface profiler (Veeco; Dektak 150), where the measurement was performed at 10 points spaced ~1 mm apart, whose average was employed. The thickness of all samples was

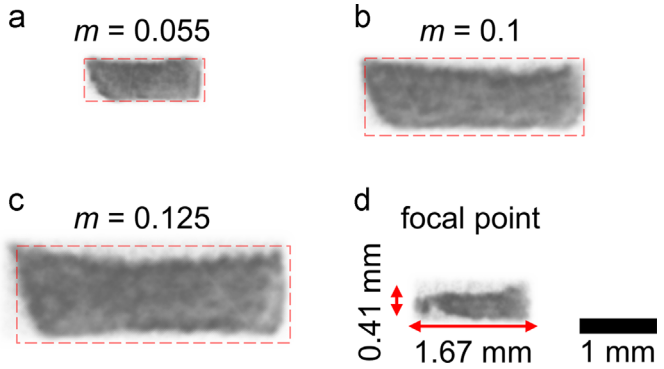

Fig. 2. Patterns of the ablation laser during the projection method recorded on thermal paper placed at the target position for the three magnifications of (a) 0.055, (b) 0.1, and (c) 0.125, projecting the rectangular slit of $L_1=2$ cm and $L_2=1$ cm. The red dashed boxes represent the ideal shapes of the projected ablation laser for (Eqs. (1) and 2). (d) Reference pattern when the ablation laser is focused onto the thermal paper at a distance of the focal length without any slits, which is the typical laser spot shape on the target during conventional pulsed laser deposition.

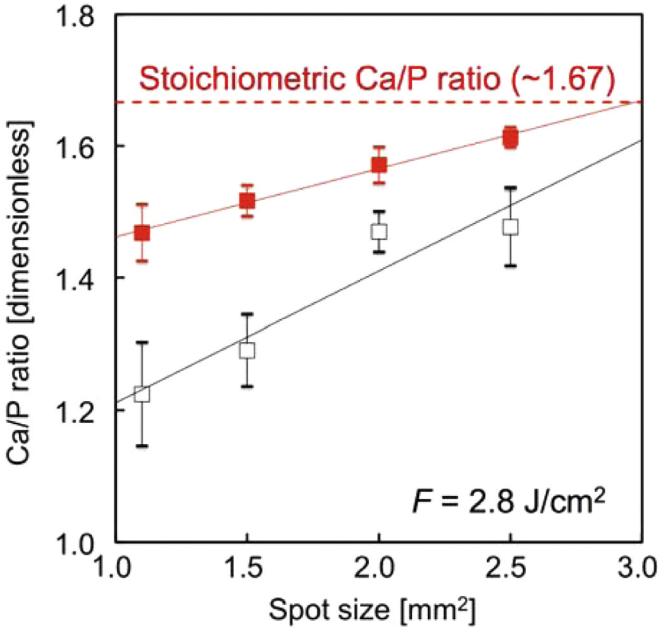

Fig. 3. The Ca/P ratio of the HA thin films for various spot sizes with the defocus method (black open squares) and the projection method (red solid squares), with solid lines to guide the eye. The error bars are the standard errors. The fluence is fixed at $F=2.8$ J/cm^2. It is found that a larger spot size improves the Ca/P ratio in both methods, though the projection method generates a much better HA thin film with respect to the Ca/P ratio. The stoichiometric Ca/P ratio of 1.67 is shown with a dashed red line.

within $(5.0 \pm 0.5) \times 10^2$ nm^2. The Ca/P ratio of the HA thin films was measured by X-ray photoelectron spectroscopy (ULVAC-PHI; PHI X-tool, Al Kα). The measurement was performed for Ca 2p and P 2p. The Ca/P ratio data were averaged for three different samples for each *ss*.

3. Results and discussion

Fig. 2 shows examples of the laser spots as viewed on thermal paper placed at the same position of the target. We obtained the spots shown in Fig. 2(a), (b) and (c) with $m=0.055$, $m=0.1$ and $m=0.125$, respectively. The distortion of the spot shape comes from a slight bending of the thermal paper. Fig. 2(d) is the typical spot shape on the target during conventional PLD as a reference.

Fig. 3 shows the Ca/P ratio as a function of the *ss* using the defocus method and the projection method in the case where $F=2.8$ J/cm^2. The error bars are the standard errors. The dependence of the Ca/P ratio upon the *ss* provides useful information for preparing stoichiometric HA thin films where the Ca/P ratio = 1.67. It is clearly seen that a larger *ss* exhibits better Ca/P ratios for both methods. The result that a better Ca/P ratio can be obtained with a larger *ss* agrees with our previous study [19], though the signs of the slopes of Ca/P vs. *ss* are opposite. Specifically, the Ca/P ratio was found to decrease with the *ss* and the Ca/P ratio was larger than stoichiometry in the previous study. The reason for these differences is not understood at present, though differences in the experimental conditions may be possible explanations. For instance, the substrate in this study was Al_2O_3 (0001) used at a growth temperature of 400 °C, while Ti was the substrate used at room temperature in the previous study. These differences may affect the Ca/P ratio via the sticking coefficient of the ablated chemical species. The difference of the partial pressures (0.1 Pa for the previous study and 50 Pa for this study) will also affect the Ca/P ratio by changing the conditions of the flight of the atoms via collisions and chemical reaction processes with the gas molecules. These differences should be studied in future.

It is found that a larger *ss* improves the Ca/P ratio for both methods and the projection method improves the Ca/P ratio. We consider that both of these results are related to the uniformity of the spatial energy distribution of the ablation laser. Because the fluence is held constant in this study, a larger *ss* should yield a lower energy at each spatial position, which will lead to a more uniform spatial energy distribution of the ablation laser. The spatial energy distribution of the ablation laser in the projection method is more uniform than that in the defocus method because the weak portion of the ablation laser is removed. Therefore, the results indicate that the uniformity of the ablation laser is the factor to prepare stoichiometric HA thin films by PLD.

4. Conclusion

Two methods were examined to study the dependence of the Ca/P ratio upon the spot size and the spatial energy distribution of an ablation laser with a constant fluence, i.e., the defocus method and the projection method. A larger spot size improved the Ca/P ratio with both methods, though the projection method drastically improved the Ca/P ratio compared to the defocus method. Under a constant fluence, the spatial energy distribution of the ablation laser was more uniform with larger spot sizes for both methods, and was more uniform for the projection method than the defocus method. It is considered that these improvements of the Ca/P ratio arise from the improved uniformity of the spatial energy distribution of the ablation laser.

Acknowledgments

This work was supported in part by a grant from the Strategic Research Foundation Grant-aided Project for Private Universities from the Ministry of Education, Culture, Sports, Science, and Technology, Japan, 2013–2017 (No. S1311045) and a grant from the Project Research of the Faculty of Biology-Oriented Science and Technology, Kinki University, 2015-2016 (No. 14-I-3).

References

[1] R.G.T. Geesink, K. De Groot, C.P.A.T. Klein, Chemical implant fixation using

hydroxyl-apatite coatings, Clin. Orthop. Relat. Res. 225 (1987) 147–170.
[2] C.P.A.T. Klein, P. Pakta, H.B.M. Van der Lubbe, J.G.C. Wolke, K. De Groot, Plasma-sprayed coatings of tetracalciumphosphate, hydroxyl-apatite, and α-TCP on titanium alloy: an interface study, J. Biomed. Mater. Res. 25 (1991) 53–65.
[3] R. McPherson, N. Gane, T.J. Bastow, Structural characterization of plasma-sprayed hydroxylapatite coatings, J. Mater. Sci. Mater. Med. 6 (1995) 327–334.
[4] W.Q. Yan, T. Nakamura, K. Kawanabe, S. Nishigochi, M. Oka, T. Kokubo, Apatite layer-coated titanium for use as bone bonding implants, Biomaterials 18 (1997) 1185–1190.
[5] A. Stoch, A. Brożek, G. Kmita, J. Stoch, W. Jastrzębski, A. Rakowska, Electrophoretic coating of hydroxyapatite on titanium implants, J. Mol. Struct. 596 (2001) 191–200.
[6] S. Hontsu, M. Nakamori, H. Tabata, J. Ishii, T. Kawai, Pulsed laser deposition of bioceramic hydroxyapatite thin films on polymer materials, Jpn. J. Appl. Phys. 35 (1996) L1208–L1210.
[7] H. Nishikawa, R. Hatanaka, M. Kusunoki, T. Hayami, S. Hontsu, Preparation of freestanding hydroxyapatite membranes with excellent biocompatibility and flexibility, Appl. Phys. Express 1 (2008) 088001.
[8] Y. Sakoishi, R. Iguchi, H. Nishikawa, S. Hontsu, T. Hayami, M. Kusunoki, C-axis-oriented hydroxyapatite film grown using ZnO buffer layer, Appl. Phys. Express 6 (2013) 115501.
[9] J.L. Ong, L.C. Lucas, W.R. Lacefield, E.D. Rigney, Structure, solubility and bond strength of thin calcium phosphate coatings produced by ion beam sputter deposition, Biomaterials 13 (1992) 249–254.
[10] M. Yoshinari, T. Hayakawa, J.G. Wolke, K. Nemoto, J.A. Jansen, Influence of rapid heating with infrared radiation on RF magnetron-sputtered calcium phosphate coatings, J. Biomed. Mater. Res. 37 (1997) 60–67.
[11] A.M. Ektessabi, H. Kimura, Characterization of the surface of bio-ceramic thin films, Thin Solid Films 270 (1995) 335–340.
[12] H. Zeng, K.K. Chittur, W.R. Lacefield, Dissolution/reprecipitation of calcium phosphate thin films produced by ion beam sputter deposition technique, Biomaterials 20 (1999) 443–451.
[13] K. Yamashita, T. Arashi, K. Kitagaki, S. Yamada, T. Umegaki, K. Ogawa, Preparation of apatite thin films through rf-sputtering from calcium phosphate glasses, J. Am. Ceram. Soc. 77 (1994) 2401–2407.
[14] J.G.C. Wolke, K. Van Dijk, H.G. Schaeken, K. De Groot, J.A. Jansen, Study of the surface characteristics of magnetron-sputter calcium phosphate coatings, J. Biomed. Mater. Res. 28 (1994) 1477–1484.
[15] M. Okazaki, T. Aoba, Y. Doi, J. Takahashi, Y. Moriwaki, The effect of the calcium-phosphate feed molar ratios on apatite formation, J. Osaka Univ. Dent. Sch. 19 (1979) 87–93.
[16] M. Tyunina, S. Leppävuori, Effects of laser fluence, size, and shape of the laser focal spot in pulsed laser deposition using a multielemental target, J. Appl. Phys. 87 (2000) 8132–8142.
[17] T. Ohnishi, M. Lippmaa, T. Yamamoto, S. Meguro, H. Koinuma, Improved stoichiometry and misfit control in perovskite thin film formation at a critical fluence by pulsed laser deposition, Appl. Phys. Lett. 87 (2005) 241919.
[18] J.H. Song, T. Susaki, H.Y. Hwang, Enhanced thermodynamic stability of epitaxial oxide thin films, Adv. Mater. 20 (2008) 2528–2532.
[19] H. Nishikawa, R. Yoshikawa, Controlling the chemical composition of hydroxyapatite thin films using pulsed laser deposition, Trans. Mater. Res. Soc. Jpn. 40 (2015) 111–114.
[20] V. Kekkonen, A. Hakola, T. Kajava, Diffractive shaping of excimer-laser beams for pulsed laser deposition, J. Eur. Opt. Soc. Rapid 6 (2011) 11013s.